Effect of Drying Conditions on Drying Rate and Physical Properties of a Porous Solid

E. H. Lebeis and T. A. Burtis
Houdry Process Corporation, Marcus Hook, Pennsylvania

Rate data are presented for both the constant – and the falling-rate drying of closely sized spheres of silica-alumina hydrogel. This hydrogel, which contains a fine powder, is the starting material from which petroleum cracking catalysts may be prepared. During the constant-rate period the drying rate is directly proportional to the difference between the dry- and wet-bulb temperatures of the air. In the falling-rate period the rate is proportional to the free water content, the proportionality factor being an undetermined function of the dry-bulb–wet-bulb differential.

Drying severity during the falling-rate period is shown to be the major determinant of the final pellet density. At constant wet-bulb temperature, density is inversely related to the dry-bulb–wet-bulb differential. If this differential is held constant, density is directly related to the wet-bulb temperature.

The variation in drying rate with position in the bed for through-circulation constant-rate drying of deep beds of particles is analyzed for the case where the direction of air flow is periodically reversed for equal time intervals. It is indicated that uniformity of drying should increase with an increase in air velocity, but decrease as bed depth is increased. At constant conditions and bed depth, large particles should dry more uniformly than small. Within normal operating ranges, air temperature and humidity should have little effect on drying uniformity.

In chemical processes in which solid catalysts are required, the physical as well as the catalytic properties of the solid are of great importance. This is especially true of petroleum cracking catalysts prepared from hydrogels. The properties of the final product are usually dependent upon the drying conditions employed. In the drying of hydrogels, from 5 to 15 lb. of water must be evaporated for every pound of catalyst produced. Drying equipment and operating costs therefore are generally high. This paper presents the results of an experimental study of the drying of spherical hydrogel catalyst particles undertaken to obtain basic rate data for equipment selection and design and to explore the effects of drying conditions on the physical properties of the catalyst.

When small particles of this type are dried by through circulation of air, the material is usually spread in a relatively deep multilayer bed (4). By use of this technique, a fairly high degree of heat economy can be achieved because the dry-bulb temperature of the air leaving the bed closely approaches the wet-bulb temperature. However, because of this change in dry-bulb temperature as the air passes through the bed, there is considerable variation in drying rate from one side of the bed to the other in this type of operation.

In order to eliminate this variation in the laboratory, the experimental work was limited to the drying of a single layer of particles. A small-scale dryer was built specifically for this program. The drying-rate data obtained should, strictly speaking, be applicable only

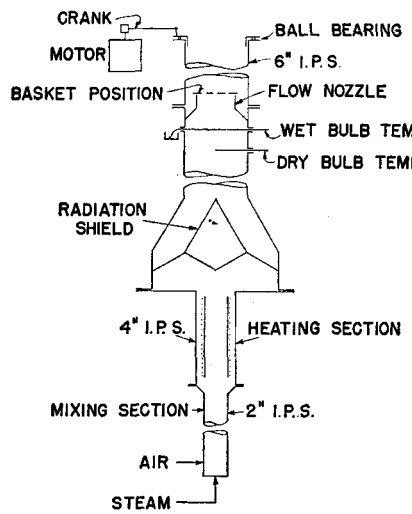

Fig. 1. Sectional view of dryer.

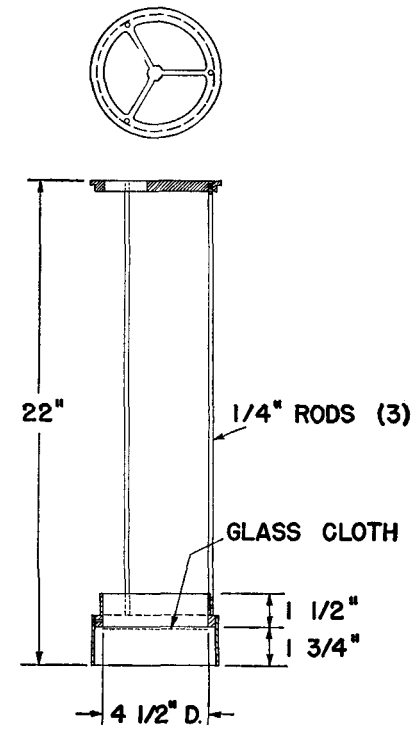

Fig. 2. Detail of dryer basket.

E. H. Lebeis is at present affiliated with Catalytic Construction Company, Philadelphia, Pennsylvania.

to single layers and not to deeper beds, as heat and mass transfer rates will differ somewhat for multiple layers because of the difference in air turbulence. For design purposes, however, the use of single-layer data is conservative. A method is given for predicting the degree of drying uniformity obtainable with multilayer beds. The effects of particle size, air velocity, temperature, and bed depth are discussed.

EQUIPMENT AND OPERATING PROCEDURE

A sectional drawing of the experimental dryer is shown in Figure 1. Metered quantities of preheated air and steam were introduced to the bottom section, which served as a mixing chamber. The mixed stream then flowed upward over an electrical heating element, which raised the temperature to the desired dry-bulb level.

A baffle was placed above this section to serve as a radiation shield between the material being dried and the heating element. Above this baffle the air dry- and wet-bulb temperatures were measured. The air was then passed through the layer of hydrogel spheres, or beads, and discharged from the dryer.

The basket in which the charge was suspended is shown in detail in Figure 2. The beads rested upon an open-meshed "leno-weave" glass cloth of 13 by 25 mesh. Glass cloth was used to minimize heat transfer by conduction. The glass cloth was held in place by a skirt which extended below the level of the glass cloth. This skirt fitted down inside the flow nozzle shown in Figure 1 when the basket was in the dryer, an arrangement that prevented air from bypassing the beads. In some runs the space into which the skirt extended was filled with Dow silicone fluid of very high boiling point to provide a liquid seal. The presence or absence of fluid had no discernible effect on drying rates, which indicated that little air was by-passed when the apparatus was operating with a dry seal.

The basket proper was rigidly connected to a ring above by three rods. The top ring fitted into the race of a ball bearing mounted at the top of the dryer. A small motor and crank imparted to the ball bearing a reciprocating rotary motion, which was in turn imparted to the top ring and, through the rods, to the basket below. This motion effectively agitated the beads to promote drying uniformity.

The top ring and basket were fabricated from aluminum. The basket skirt was formed from light-gauge 18-8 stainless steel. The rods which connected ring and basket were Dowmetal. These metals satisfactorily combined corrosion resistance and light weight.

Standard steel pipe was used for the dryer shell, and the inside surfaces were painted with aluminum paint to retard both corrosion and radiation.

External electrical heating circuits were provided at the top of the dryer to prevent condensation on the walls during high humidity runs. The steam transfer line connecting the metering orifice with the dryer was similarly wired to avoid condensation in the line and to provide some superheat. The compressed-air feed was preheated in a steam-jacketed double-pipe heat exchanger.

The operating procedure was as follows. The dryer was heated on air alone until the dry-bulb temperature exceeded the wet-bulb temperature to be employed. Steam flow was then started. The steam and air flow rates were set to give the desired total flow rate and wet-bulb temperature. When all temperatures, including those at the wall, were lined out, the basket containing the wet beads was lowered into place without cessation of air or steam flow. At the end of the drying period the basket was removed, again without stopping the flow.

The beads were weighed before and after each run. The unit was originally set up to weigh the basket and beads during the run, but it was found impossible to weigh accurately with air flowing. Stopping the air flow during the time of weighing produced undesirable temperature fluctuations. The best method found for obtaining reliable drying-rate data was to dry successive batches of the same charge for various times, discharging the product immediately into airtight weighing bottles.

The solid studied in this investigation was a silica-alumina hydrogel prepared essentially according to a method which has been previously described(*3*). A feature of this method is the incorporation of finely ground dried gel powder in the hydrogel. This powder reduces the amount of breakage in drying and helps to create large pores, or macropores, in the catalyst structure. In the absence of this powder the catalyst would contain only micropores smaller than 1,000 Å. in radius. With the powder present, pores larger than 1,000 Å. may be created during the drying operation. These large pores are desirable because, among other things,

TABLE 1.—SUMMARY OF DRYING DATA

	Primary drying conditions				Secondary drying conditions				Heat-treated properties	
Run	Dry bulb, °F.	Wet bulb, °F.	Time, min.	H_2O, wt. %	Dry bulb, °F.	Wet bulb, °F.	Time, min.	H_2O, wt. %	Porosity, vol. %	Pellet density, g./cc.
4	220	160	15	224	220	160	60	9.9	61.1	0.928
5	200	160	15	..	200	160	60	12.4	60.0	0.963
7	240	180	13	308	240	180	46	7.5	61.5	0.932
8	190	150	18	319	190	150	35	28.3	60.1	0.968
9	180	140	18	265	180	140	40	24.2	61.6	0.952
10	200	140	15	292	200	140	26	25.7	61.7	0.948
11	210	150	13	312	210	150	27	..	60.8	0.953
13	160	140	31	389	160	140	100	42.8	54.7	1.050
14	170	140	25	353	170	140	80	22.1	58.2	0.974
15	170	150	30	400	170	150	100	52.0	60.5	0.993
16	180	150	22	393	180	150	100	17.0	58.1	0.989
17	180	150	22	386	245	212	80	21.9	58.1	1.051
18	180	150	25	364	180	150	100	16.6	61.0	0.957
19	180	150	25	359	210	150	45	10.6	62.5	0.920
20	180	150	25	336	210	180	80	19.8	59.1	1.006
21	180	150	25	350	240	180	45	9.0	61.3	0.948
22	180	150	25	338	272	212	45	10.6	58.0	1.01
23	210	150	13	325	180	150	100	14.3	60.4	0.955
24	210	150	13	336	210	150	47	7.7	61.5	0.917
25	210	150	13	314	210	180	80	16.7	56.9	1.023
26	210	150	13	322	240	180	40	10.5	59.3	0.973
27	210	150	13	316	242	212	80	22.9	56.8	1.046
28	210	150	13	309	272	212	45	9.5	57.2	1.034

they increase the speed of regeneration when coke is burned from used catalyst. As charged to drying, this material has the consistency of very stiff, elastic gelatin.

Because the particles were formed as very regular, slightly flattened spheres, it was possible to obtain a very closely sized fraction by screening. The effect of particle diameter on drying rate was eliminated by using one size of fraction throughout the study. The major diameter of the beads charged to the dryer varied from 8.5 to 10.5 mm., the average being 9.6 mm. The diameter of the completely dried beads was about one half this figure. The water content of the wet beads averaged 6.40 lb./lb. of dry gel. Moisture contents were determined by measuring the weight loss of a sample after 16 hr. in a standard laboratory drying oven in an air atmosphere at 220°F. All moistures are expressed on the dry at 220°F. basis.

All runs were made at an air velocity of 200 std.cu.ft./sq.ft. of bed/min. The drying was separated into two stages in order to differentiate between the constant- and the falling-rate periods. The first drying stage was terminated when the water content had reached about 3.0 lb./lb. of dry gel. Earlier work had shown that the critical moisture content at which the rate changed from constant to falling was about 1.5 lb./lb. of dry gel. In the second drying stage the water content was lowered from approximately 3.0 to between 0.1 and 0.2 lb./lb., which is close to the equilibrium water content.

Physical properties of the beads were studied after calcination. Porosity and pellet density were determined by measurement of the volume of water absorbed and of the volumetric displacement of the water-soaked beads. Large-pore volume was determined by measuring the volume of mercury absorbed by previously evacuated catalyst under 1,000 lb./sq.in. gauge pressure. This method gives the volume of the pores larger than 1,000 Å. in radius.

DISCUSSION OF EXPERIMENTAL RESULTS

Drying Rates

A summary of drying data is presented in Table 1. In the first series of experiments (runs 4 to 16, Table 1) the effects of air temperature and humidity on the first-stage drying rates were studied. Because the drying rates were very high, no attempt was made to obtain incremental rate data. Drying times varied between 13 and 31 min., depending upon the conditions employed. The over-all drying rates were obtained by subtracting the moisture content of the discharged beads from that of the charge and dividing by the drying time.

The results of these experiments are shown in Figure 3, where the first-stage drying rate is plotted vs. the difference between dry- and wet-bulb temperature. It can be seen that drying rate is directly proportional to this temperature difference. The fact that the line passes through the origin shows that the bead temperature must be close to the air wet-bulb temperature or, in other words, that air-to-solid temperature-driving force approximates the difference between dry- and wet-bulb temperatures.

In order to aid in determining the drying mechanism, beads discharged from the first-stage operation were visually examined before and after being immersed in water. The discharged beads were similar

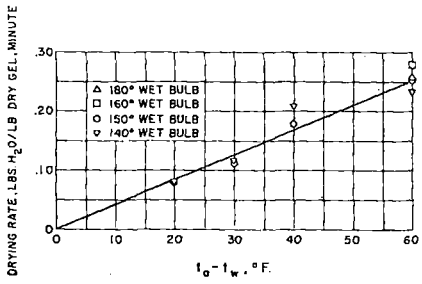

Fig. 3. Primary drying rate vs. dry-bulb—wet-bulb temperature difference.

in translucence to the charged beads, although they were smaller in size. No pickup of water or displacement of air was apparent on immersion in water. These facts show that no vapor spaces had been created within the structure during this part of the drying operation. In the absence of internal vapor spaces evaporation had to take place only from the outside surface, and water removal was accompanied by shrinkage of the bead. Had any evaporation occurred within the structure, a diffusional resistance large in relation to the resistance of the gas film would have been imposed. In this case the diffusion rate and therefore the drying rate would be influenced by the wet-bulb temperature. The fact that no significant variation of drying rate with wet-bulb temperature can be noted in Figure 3 is a further indication that no internal vapor diffusion occurred. The effect of wet-bulb temperature on the gas-film transfer coefficients was apparently less than the experimental error.

Drying-rate data during the second stage were taken at two sets of conditions. In both cases the wet-bulb temperature was maintained at 180°F. In one case the dry-bulb temperature was 240°F.; in the other, 210°F. Samples from successively longer drying runs were weighed and analyzed for moisture content. In addition, the diameter was measured. At each set of conditions one sample was held in the dryer until its weight was constant. The moisture content of this sample was taken as the equilibrium moisture content. The moisture analyses were then converted from total moisture on the dry at 220°F. basis to free moisture on the equilibrium dry basis.

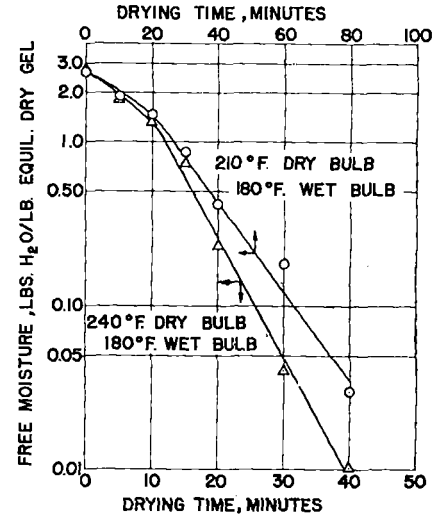

Fig. 4. Secondary drying curves.

The data obtained in these two runs are plotted in Figure 4. Free-moisture content is plotted vs. time. These curves follow the normal pattern closely. On semilog paper a curve should be obtained during the period when drying rate is constant. After the critical moisture content is passed and the drying rate falls with moisture content, a straight line should be obtained, provided drying rate is strictly proportional to moisture content. The exact location of the critical point is not obvious by inspection of the curves, but it appears to be in the neighborhood of a moisture content of 1.5 lb. water/lb. of equilibrium dry gel.

The drying rates in the falling-rate period can be expressed in the form (*5*)

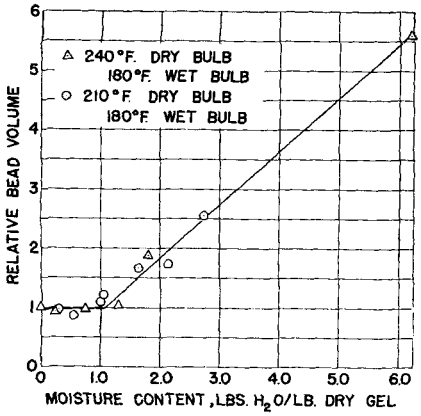

Fig. 5. Bead shrinkage during drying.

$$\frac{dW}{d\theta} = -k(W - W_e)$$

where k is the slope of the straight lines in Figure 4. The value of k for the run at 60°F. differential between dry- and wet-bulb is about 2.7 times the value at 30°F. differential, an indication that although k is related to this differential, it is not directly proportional. Further study is needed to define the relationship. A possible explanation is that evaporation takes place in both runs at a temperature higher than the wet-bulb temperature.

The shrinkage data taken in these runs are plotted in Figure 5, where relative bead volume is plotted against moisture content. The data show that shrinkage is linear with moisture content until a moisture content between 1.0 and 1.5 has been reached. Below this range shrinkage is less than can be picked up by this test. In the absence of a significant amount of shrinkage, the water removal must be from pores within the structure.

These data, together with the drying-rate curves, indicate that the critical moisture content is between 1.0 and 1.5. Down to this point shrinkage keeps pace with drying and so all evaporation is from the surface and the rate is essentially constant. Below the critical there is little shrinkage and evaporation is from internal pores. The rate falls as the diffusional resistance is increased.

Effect of Drying Conditions on Physical Properties

A series of twelve experiments (runs 17 to 28, Table 1) was made to determine the effect of drying conditions on the final physical properties of the beads. Two first-stage drying conditions were employed. Six runs were made at 180°F. dry bulb, 150°F. wet bulb, and 25 min. drying time. The other six runs were made at 210°F. dry bulb, 150°F. wet bulb, and 13 min. drying time. Six sets of second-stage drying conditions were selected. The samples originally slow-dried and those originally fast-dried were both finally dried at these six final drying conditions. Three wet-bulb temperatures were used: 150°, 180°, and 212°F. At each wet-bulb level two dry-bulb temperatures were used, one 30°F. above the wet bulb, and one 60°F. above the wet bulb. With the 30° differential the drying time was 80 to 100 min.; with the 60° differential the drying time was 45 min.

The results of these experiments are given in Table 2. The runs are grouped by wet-bulb temperature level at which the secondary drying was conducted. It can be seen that at each secondary drying condition essentially the same density and porosity were obtained with those originally slow-dried as with those originally fast-dried. This indicated that the drying conditions during the constant-rate period had relatively little effect.

The conditions during the falling-rate period, however, had profound effects on the final bead-catalyst density. At each wet-bulb level the density is higher for the sample dried at the lower dry-bulb temperature, that is, dried at the lower rate. At constant temperature difference between dry and wet bulb the density increases as the wet-bulb temperature is raised. All the density variations noted can be explained by the changes in porosity within the limits of experimental error.

Included in Table 2 are large-pore data for some of the catalysts. It is apparent that some relationship exists between density and large-pore volume. To determine that relationship better, the large-pore-volume data were used to calculate the gel density, which is the pellet density that would be obtained if no large pores were present. The formula used is

$$\text{gel density} = \frac{1}{\frac{1}{\text{pellet density}} - \text{large-pore volume}}$$

The gel densities calculated for those samples for which large-pore data were available are given in Table 3. The data are arranged in order of increasing pellet density and decreasing large-pore volume. The uniformity of the calculated gel-density values indicates that practically all the pellet density variation is the result of differences in large-pore volume.

The conclusion is drawn that increasing the drying severity, either by increasing the dry-bulb temperature at constant wet-bulb temperature or by decreasing the wet bulb at any given differential between dry and wet bulb, results in greater structural strains in drying. The physical manifestation of the greater strain is increased large-pore volume and decreased pellet density. In order to obtain a particular catalyst density, the permissible drying rate is a function of the wet-bulb temperature. The higher the wet-bulb temperature, the faster the catalyst may be dried. Because this material is so sensitive to drying conditions in the falling-rate period, it is evident that the drying conditions must be kept as uniform as possible in order to produce a high-quality product.

TABLE 3.—GEL DENSITIES CALCULATED FROM LARGE-PORE VOLUMES

Pellet density, g./cc.	Large-pore vol., cc./g.	Calc. gel density, g./cc.
0.917	0.14	1.05
0.957	0.12	1.08
0.973	0.09	1.07
1.034	0.03	1.07
1.051	0.01	1.06

TABLE 2.—EFFECT OF DRYING CONDITIONS ON PHYSICAL PROPERTIES

Secondary drying conditions		Slow primary drying(*)			Fast primary drying(†)		
Dry-bulb temp., °F.	Wet-bulb temp., °F.	Pellet density, g./cc.	Porosity, vol. %	Large pore vol., cc./g.	Pellet density, g./cc.	Porosity, vol. %	Large pore vol., cc./g.
210	150	0.920	62.5	..	0.917	61.5	0.14
180	150	0.957	61.0	0.12	0.955	60.4	
240	180	0.948	61.3	..	0.973	59.3	0.09
210	180	1.006	59.1	..	1.023	56.9	
272	212	1.01	58.0	..	1.034	57.2	0.03
242	212	1.051	58.1	0.01	1.046	56.8	

*Slow drying—180°, dry bulb, 150°F. wet bulb, 25 min.
†Fast drying—210°F. dry bulb, 150°F. wet bulb, 13 min.

This study shows, then, that the drying operation could logically be divided into two separate operations: a primary stage in which the catalyst is rapidly dried at a relatively low wet-bulb level and a secondary stage in which the catalyst is further dried at as high a wet-bulb temperature as possible and at a rate which will give the desired physical properties. The main reason for this separation of operations is that corrosion of the dryer becomes increasingly severe as the wet-bulb temperature is raised. Therefore, cheaper construction can be used for the low wet-bulb primary stage than for the higher wet-bulb secondary stage. The exact wet-bulb temperature at which the secondary drying is performed is selected by an economic balance which considers both the effect of wet bulb on material costs and the effect of rate on dryer size.

It is obviously desirable to evaporate as much water as possible in the cheaper first-stage dryer. On the other hand, it is also essential that no particle be dried past the critical moisture content at these relatively severe drying conditions. Because this portion of the drying operation must be stopped before the fastest drying particle reaches the critical moisture content, uniformity of drying becomes a factor of great importance. Stated another way, total dryer investment cost will be lowest when when maximum drying uniformity is achieved in the first stage of operation. Even for more conventional single-stage drying operations, uniformity is important, as the dryer must be sized to lower the moisture content of the slowest drying particle to the desired level. Therefore, the following analysis of the factors influencing uniformity of drying during the constant-rate period was made. It has been shown that uniformity during the falling-rate period is also essential. Although an analysis was not made for the falling-rate period, many of the conclusions may be applied to that period.

UNIFORMITY OF DRYING IN DEEP BEDS

It was previously mentioned that materials of the type studied in this investigation are often dried commercially in moving-belt tunnel dryers by circulation of heated air through relatively deep beds. The bed thickness is usually between ½ and 3 in. Reversal of the direction of air flow through the bed in successive zones is frequently practiced. This technique materially minimizes the nonuniformity of drying through the bed. The analysis which follows is based upon this reversing-flow technique for the constant-rate period.

The first case to be considered is that of air flow in one direction only. It is assumed that air flows upward through the bed. The amount of heat transferred per hour in a square foot of bed of unit thickness may be expressed as

$$\frac{q}{A} = G c_p \Delta t_a \qquad (1)$$

when the relatively small amount of sensible heat imparted to the vaporized water is neglected. The amount of heat transferred is also related to the heat transfer coefficient as follows:

$$\frac{q}{A} = \frac{(ha)\, L' \Delta t_m}{12} \qquad (2)$$

where

$$\Delta t_m = \frac{\Delta t_1 - \Delta t_2}{2.3 \log \Delta t_1 / \Delta t_2} \qquad (3)$$

and

L' = bed thickness, in.

If, in accordance with the findings of this investigation, the solid temperature is constant and equal to the air wet-bulb temperature,

$$\Delta t_a = \Delta t_1 - \Delta t_2 \qquad (4)$$

Substituting this value in Equation (3) gives

$$\Delta t_m = \frac{\Delta t_a}{2.3 \log \Delta t_1 / \Delta t_2} \qquad (5)$$

Combining Equations (1), (2), and (5) and solving for $\log \Delta t_1 / \Delta t_2$ yield

$$\log \frac{\Delta t_1}{\Delta t_2} = \frac{0.0362\,(ha)\, L'}{G c_p} \qquad (6)$$

All the constants in the right-hand side of Equation (6), except L', can be evaluated by selecting the air-mass velocity and dry- and wet-bulb temperatures, provided the relationship between the heat transfer coefficient and these conditions is known. Combining these constants into one constant, C, gives

$$\log \frac{\Delta t_1}{\Delta t_2} = CL' \qquad (7)$$

It has been shown (*see* Figure 3) that drying rate during the constant-rate period is directly proportional to the difference between air dry- and wet-bulb temperatures. In accordance with the basic assumption of this derivation, the temperature of the solid may be substituted for air wet bulb. Then Δt_1 and Δt_2 are proportional to the drying rates at those points. If a value of unity is assigned to Δt_1, then Δt_2 represents the ratio of the drying rate at a point L' in. from the entrance of the bed to the drying rate at the entrance. This relationship is illustrated by the line labeled *upflow* in Figure 6.

Figure 6 was plotted by use of a value for the heat transfer coefficient of 2,100 B.t.u./(hr.)(cu. ft.)(°F.) calculated from constant-rate drying runs at the following conditions: $G = 750$ lb./(sq.ft.)(hr.), $t_a = 240$°F., $t_w = 180$°F. This value agrees well with a value calculated from a previously published correlation (*1*).

If the direction of air flow is periodically reversed for equal time intervals instead of remaining constant, the variation in drying rate with bed position may be determined for any particular bed depth by the method shown in Figure 6 where a bed 2 in. deep is assumed. Here a mirror image of the original curve is drawn to represent downflow operation. The ordinates of the two curves are then averaged to yield the concave curve representing cumulative drying-rate variation with position in the bed.

At the conditions upon which Figure 6 was calculated, the ratio of the drying rate at the center of the bed to that at the edges of the bed is $0.48/0.615 = 0.78$. It may be readily seen that the concavity of the reversing-flow curve will increase as the bed thickness is increased. This states the logical expectation that drying uniformity will suffer as the bed thickness is increased.

With reference to Equation (6), increasing the heat transfer coefficient while otherwise maintaining constant conditions will result in up- and downflow lines of greater slope in Figure 6. The reversing-flow curve will then have greater concavity. The only way to increase the heat transfer coefficient without changing air velocity, humidity, or temperature is by decreasing the particle size of the material being dried (*1* and *2*). It may be expected then that small particles will dry less uniformly than large, all conditions including bed depth being equal. It must be noted, though, that the over-all drying rate will be higher for the smaller particles.

The effect of air velocity on drying uniformity may be readily interpreted with the aid of equation (6). The heat transfer coefficient has been shown (*1*) to vary approximately as the six-tenths power of the velocity. Then

$$\log \frac{\Delta t_1}{\Delta t_2} = \varphi \frac{G^{0.6}}{G} = \varphi G^{-0.4} \quad (8)$$

indicating that an increase in air velocity should result in more uniform drying. The maximum velocity is dictated by pressure-drop considerations.

The effect on drying uniformity of varying bed thickness with reversal of air flow is best illustrated by Figure 7. This curve was derived as follows. Equation (7) was converted to

$$\Delta t_2 = \frac{\Delta t_1}{e^{C'L'}} \quad (9)$$

where $C' = 2.303C$. The relative drying rate at the center of the bed is proportional to

$$\Delta t_{0.5L} = \frac{\Delta t_1}{e^{0.5\ C'L'}} \quad (10)$$

Likewise, at either edge of the bed the relative drying rate with reversal is proportional to the average of Δt_1 and Δt_2 for unidirectional flow, or

$$\frac{\Delta t_1 + \Delta t_2}{2} = \frac{\Delta t_1 + \Delta t_1/e^{C'L'}}{2} \quad (11)$$

Calling the ratio of drying rate at the center of the bed to that at either edge R, dividing Equation (10) by (11), and simplifying give

$$R = \frac{2}{e^{0.5\ C'L'} + e^{-0.5\ C'L'}} = \operatorname{sech}\ 0.5\ C'L' \quad (12)$$

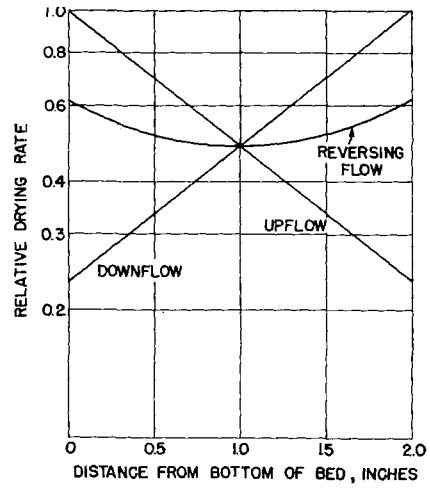

Fig. 6. Drying rate vs. position in a 2-in.-deep bed (through circulation).

R may then be readily plotted vs. L'.

The same type of analysis has not been applied to the falling-rate period; however the various factors should have the same qualitative effect as in the constant-rate period. The fact that drying rate falls as the moisture content falls has a compensating effect which should tend to make the falling-rate drying inherently more uniform than the constant-rate drying.

Although experimental confirmation of the findings of this analysis is not available, it is believed that they may be used qualitatively with confidence. The selection of drying equipment requires considerable experimental work. If uniformity of drying is a consideration, the method can be used to indicate the practical limits of operating conditions and to indicate the qualitative effect of each variable. Limiting the field can significantly decrease the amount of experimental work necessary.

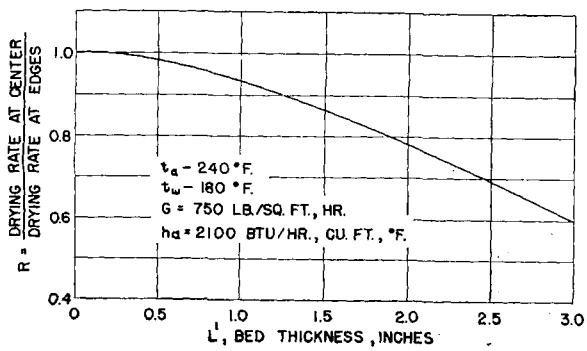

Fig. 7. Drying rate vs. bed thickness (through circulation with reversal of air flow).

CONCLUSIONS

1. The drying rate of the hydrogel studied is proportional to the difference between air dry- and wet-bulb temperatures during the constant-rate period.

2. During the falling-rate period the rate is proportional to the free-moisture content. The proportionality factor is a complicated and undetermined function of the difference between dry- and wet-bulb temperatures.

3. Wet-bulb temperature level and drying rate during the falling-rate period are the major determinants of the density and large-pore volume of cracking catalysts prepared from this hydrogel. The higher the wet-bulb temperature, the faster the catalyst may be dried to obtain the desired density.

4. According to theoretical analysis, the important factors influencing uniformity of drying during the constant-rate period when deep layers are dried are bed depth, air velocity, and particle size.

ACKNOWLEDGEMENT

The aid of E. H. Ivey, Jr., and J. B. Holiman is gratefully acknowledged. Permission by Houdry Process Corporation to publish this paper is appreciated.

NOTATION

a = surface area, sq.ft./cu.ft.
c_p = specific heat, B.t.u./(lb.) (°F.)
h = heat transfer coefficient, B.t.u./(hr.) (sq.ft.) (°F.)
k = a constant
q = heat transfer rate, B.t.u./hr.
Δt_a = change in air temperature passing through bed, °F.
Δt_1 = temperature difference between air and solid at entrance of bed, °F.
Δt_2 = temperature difference between air and solid at exit of bed, °F.
A = bed area normal to flow, sq.ft.
C, C' = constants
G = mass velocity, lb./(hr.) (sq. ft.)
L' = bed thickness, in.
W = moisture content, lb. H_2O/lb. bone dry solid
W_e = equilibrium moisture content, lb. H_2O/lb. bone dry solid
θ = time, hr.

LITERATURE CITED

1. Gamson, B. W., G. Thodos, and O. A. Hougen, *Trans. Am. Inst. Chem. Engrs.*, 39, 1 (1943).
2. Marshall, W. R., Jr., and O. A. Hougen, *Trans. Am. Inst. Chem. Engrs.*, 38, 91 (1942).
3. Milliken, T. H., Jr., U. S. Pat. 2,487,065 (Nov. 8, 1949).
4. Perry, J. H., ed., "Chemical Engineers' Handbook," p. 823, McGraw-Hill Book Company, Inc., New York (1950).
5. *Ibid.*, p. 807.

Presented at A.I.Ch.E. New York meeting